Recombinant EWS-FLI1 Oncoprotein Activates Transcription†

Aykut Üren,*,‡ Olga Tcherkasskaya,§ and Jeffrey A. Toretsky‡

Lombardi Comprehensive Cancer Center, Georgetown University Medical Center, Research Building, Room W316, 3970 Reservoir Road, N.W., Box 571469, Washington, DC 20057-1469, and Department of Biochemistry and Molecular Biology, Georgetown University School of Medicine, Washington, DC 20057

Received June 11, 2004; Revised Manuscript Received August 5, 2004

ABSTRACT: The Ewing's sarcoma family of tumors (ESFT) contains a characteristic translocation the chimeric transcript of which is translated to become the EWS−FLI1 fusion protein. EWS−FLI1 regulates transcription and posttranscriptional splicing. Elimination of EWS−FLI1 protein from ESFT cells induces apoptosis and reduces xenograft tumor growth. Therefore the production of a biologically active recombinant EWS−FLI1 could lead to discoveries that would enhance our mechanistic understanding of ESFT. We have cloned, expressed, and purified a biologically active recombinant EWS−FLI1 in *Escherichia coli* using affinity column chromatography. A refolding procedure was required to render the recombinant EWS−FLI1 soluble in relatively native conditions. The structural alterations induced by the refolding procedure were monitored by SDS-gel electrophoresis, circular dichroism, and steady-state fluorescence spectroscopy. Recombinant EWS−FLI1 under native conditions approaches a largely unfolded conformation. Recombinant EWS−FLI1 protein under native conditions specifically binds to DNA and transcribes RNA. Our biologically active recombinant EWS−FLI1 oncoprotein will be useful to identify functional molecular partners and inhibitors.

Ewing's sarcoma family of tumors (ESFT)[1] are highly malignant tumors of bone and soft tissue that occur in children, adolescents, and young adults. With a combined approach of surgery, radiotherapy, and intensive chemotherapy, patients with metastatic ESFT still have a 70% mortality rate (*1*, *2*). Fortunately, ESFT contains a unique, validated tumor target, the EWS−FLI1 translocation-generated fusion protein (*3*). More than 95% of ESFT patients have the balanced translocation t(11;22)(q24;q12) or a related rearrangement. The t(11;22)(q24;q12) combines the amino-terminus of EWS (residues 1−264) from chromosome 22 with the carboxy-terminus of FLI1 (232 carboxy-terminal residues) from chromosome 11 to form EWS−FLI1 (*3*−*5*).

EWS−FLI1 retains the conserved Ets DNA binding domain from FLI1 in the fusion protein suggesting function as a transcription factor (*3*, *6*). EWS−FLI1 modulates a diverse group of target genes by binding to specific promoters including transforming growth factor-β receptor type-II (*7*), Id2 (*8*, *9*), p21 (WAF1/CIP1) (*10*), PTPL1 (*11*), and tenascin-C (*12*). Other putative targets include EAT-2 (*13*), mE2C (*14*), manic fringe (*15*), c-myc (*16*), platelet-derived growth factor C (*17*), p57KIP (*18*), and PIM-3 (*19*). EWS−FLI1 also regulates gene expression by modulating RNA splicing as shown by alteration of an E1A splice site and interaction with U1C (*20*, *21*).

Establishing therapeutic molecular targets in oncology presents a difficult challenge. ESFT and the fusion protein EWS−FLI1 represent not only a real clinical challenge but also an opportunity to enhance knowledge of tumorigenesis since EWS−FLI1 is expressed only in tumor cells and its function is required for the malignant phenotype of ESFT. EWS−FLI1 is a well described oncogene (*22*), and depletion of EWS−FLI1 by siRNA or anti-sense oligodeoxynucleotides results in inhibition of ESFT growth (*23*−*25*). Therefore, EWS−FLI1 constitutes a potential molecular target for treatment in ESFT patients. Unfortunately, more than a decade has passed since discovery of EWS−FLI1, but no clinically applicable anti-EWS−FLI1 agent has been developed.

Small molecule inhibitors of EWS−FLI1 function would likely provide very targeted ESFT therapy with a high therapeutic index. In this study, human recombinant EWS−FLI1 was cloned, expressed, and purified in its biologically active molecular form. Structural features of EWS−FLI1 were elucidated. EWS−FLI1 binding to DNA was characterized in different molecular forms. Furthermore, a cell-free coupled transcription−translation assay was developed that allows for testing the molecular activity of the recombinant EWS−FLI1 protein. A deeper understanding of the sequence−structure relationships of EWS−FLI1 promises to enhance knowledge of oncogenic transcription and enables the design of novel therapeutic molecules.

† This study received generous support from the Children's Cancer Foundation, Dani's Foundation, and NIH Grant CA88004. Core facilities of the Lombardi Comprehensive Cancer Center provided as part of Grant P30.

* To whom correspondence should be addressed. Phone: (202) 687-9504. Fax: (202) 687-1434. E-mail: au26@georgetown.edu.

‡ Georgetown University Medical Center.

§ Georgetown University School of Medicine.

[1] Abbreviations: β-ME, β-mercaptoethanol; CD, circular dichroism; CFTT, cell-free transcription−translation; DTT, dithiothreitol; EMSA, electromobility shift assays; EDTA, ethylenediaminetetraacetic acid; ESFT, Ewing's sarcoma family of tumors; GdnHCl, guanidine hydrochloride; IPTG, isopropyl β-D-1-thiogalactopyranoside; ODN, oligodeoxynucleotides; PBS, phosphate buffer saline; PMSF, phenylmethylsulfonyl fluoride.

10.1021/bi048776q CCC: $27.50
Published on Web 00/00/0000

EXPERIMENTAL PROCEDURES

Chemicals and Solutions. Ultrapure, spectroscopic grade chemicals were purchased from Sigma (St Louis, MO) and used as received. The protein concentration was assessed by spectroscopic means using reported values of extinction coefficients of aromatic residues at 280 nm (*26*, *27*). Spectroscopic experiments were carried out at 25 ± 0.05 °C controlled by an RTE-111 Neslab water bath; pH was measured using a Radiometer PHM83. Absorbance was recorded employing a Hewlett-Packard 8452A diode array spectrophotometer. Stability of protein samples was monitored by spectroscopic means monitoring tryptophan fluorescence, the absorbance of the protein, or both at 280 and 450 nm. For all samples, no significant changes in experimental data were observed after 72 h, demonstrating that no aggregation occurred.

Antibody. Anti-FLI1 (C-19) antibody (Santa Cruz Biotechnology, Inc., Santa Cruz, CA) was raised against the carboxy-terminal domain of mouse FLI protein and has been shown to recognize EWS−FLI1 (*28*). This antibody recognizes FLI1 from mouse, rat, and human, and there is only one amino acid difference between mouse and human epitopes.

Protein Expression. We cloned the coding sequence of EWS−FLI1 into pMAL-p2g (New England Biolabs, Beverly, MA) for expression in bacterial periplasmic space, pSecTag2/Hygro for expression as a secreted protein from mammalian cells and pFASTBac1 (Invitrogen Life Technologies, Grand Island, NY) for expression in SF9 insect cells. These approaches produced neither soluble recombinant protein nor high yield. The EWS−FLI1 type I coding sequence was then cloned into the pET28a(+) (Novagen, EMD Biosciences, Inc., Madison, WI) expression vector at *Nco*I and *Hin*dIII sites. This approach deleted the amino-terminal histidine and T7 tags of the vector. EWS−FLI1 was cloned in frame with the carboxy-terminal histidine tag. BL21-CodonPlus(DE3)-RP competent cells (Stratagene, La Jolla, CA) containing the expression vector were grown overnight at 37 °C in Luria−Bertani media with 50 μg/mL kanamycin. The culture was then diluted 1:50 in 1 L of fresh Luria−Bertani media without kanamycin and allowed to grow at 37 °C until an optical density of 0.6 was observed at 600 nm. Protein production was initiated by adding 1 mM isopropyl β-D-1-thiogalactopyranoside (IPTG), and bacteria were cultured for an additional 3−4 h at 30 °C. A large scale production was performed with 100 L of bacteria in a fermentor at the University of Maryland, Bioprocess Scale-up Facility (College Park, MD). Inclusion body fraction and soluble fraction in small scale experiments were prepared by using the BugBuster protein extraction reagent (Novagen, EMD Biosciences, Inc., Madison, WI) according to the manufacturer's protocol. Inclusion body preparation from the 100 L fermentation began with French-press to break the bacterial cell wall, followed by centrifugation at 5000*g* and storage at −80 °C. A frozen pellet corresponding to 5 L of bacteria culture was resuspended in 120 mL of 20 mM Tris-HCl (pH 7.8) buffer containing 10 mM EDTA and 1% Triton X-100 (*29*). Four aliquots of sample were centrifuged at 10 000*g* for 25 min at 4 °C, resuspended in 30 mL of buffer, and centrifuged again. The insoluble fraction was washed three times, and the final pellets (inclusion body fraction) were stored at −20 °C until the day of purification.

Protein Purification. Protein purification was done according to previously published protocols (*30*, *31*). An inclusion body pellet corresponding to 1.25 L of bacterial culture was resuspended in 50 mL of 20 mM $NaPO_4$ (pH 7.8) containing 500 mM NaCl and 8 M urea. Debris was removed by centrifugation at 4000*g* for 10 min at 4 °C. The supernatant was filtered (0.22 μm pore size) and applied to a 1 mL prepacked metal chelating column on an AKTA-prime chromatography system (Amersham Biosciences, Piscataway, NJ). Initially, metal chelating columns were washed with 10 mL of H_2O, charged with 10 mL of 100 mM $NiSO_4$, washed again, and equilibrated in 10 mL of 20 mM $NaPO_4$ (pH 7.8) containing 500 mM NaCl and 8 M urea. Protein was then eluted from the column by a slow pH gradient from pH 7.8 to 4 (without changing the solvent compositions) at a flow rate of 1 mL/min at 4 °C. Aliquots (1 mL) were collected and then applied to an 8% acrylamide gel for silver staining (BioRad Laboratories, Hercules, CA) and Western blotting (*32*).

Refolding Protocol. Refolding of recombinant protein that was purified in 8M urea was tested by applying previously published methods (*29*). A series of conditions were tested for refolding of the recombinant protein from the inclusion bodies both prior to and after purification. Neither dialysis, dilution, nor additive-assisted refolding approaches resulted in refolded, soluble protein. Inclusion bodies were solubilized in 20 mM Tris (pH 7.5), 8 M urea, and 500 mM NaCl and dialyzed either directly to 20 mM Tris (pH 7.5) or stepwise to the same buffer with 4 M, 2 M, or 0.5 M urea. The same experiment was done with 150 mM NaCl instead of 500 mM or 6 M guanidine hydrochloride instead of 8 M urea. Using Tris buffer at pH 8.0 or 8.5 was not helpful. A protein refolding kit that utilizes 500 mM CAPS buffer with or without a detergent (*N*-lauroylsarcosine) also resulted in precipitated protein (Novagen, EMD Biosciences, Inc., Madison, WI) (*33*). Additionally, we tested the dialysis of purified recombinant protein into 25 mM NaPO4 (pH 7.4), 10% glycerol, 50 mM KCl, 5 mM $MgCl_2$, and 1 mM DTT directly or stepwise with 2 or 0.5 M urea in the same buffer (*31*). We also tested refolding by dialysis into the following buffers: 100 mM $NaPO_4$ (pH 7.4), 1 mM EDTA, 150 mM NaCl, 0.1 mM β-mercaptoethanol (β-ME) or 100 mM $NaPO_4$ (pH 7.4), 1 mM EDTA, 150 mM NaCl, 2 mM reduced gluthatione, and 1 mM oxidized gluthatione. Following many different approaches to obtain EWS−FLI1 in solution, reapplication of protein to a Ni^+-charged column was successful.

Immobilization-Assisted Refolding: Several fractions with high content of EWS−FLI1 in 20 mM $NaPO_4$ (pH 4.0), 500 mM NaCl, and 8 M urea were selected and pooled together. Seven to ten milliliters of pooled samples were added to 50−60 mL of the same buffer at pH 7.8; the final solution was pH 7.5 ± 0.1. A new metal chelating column was prepared as described above and then equilibrated with 10 mL of 20 mM $NaPO_4$ (pH 7.8), 500 mM NaCl, and 8 M urea. Pooled fractions from the first column were loaded followed by 10 mL of buffer (pH 7.8) wash. Column media was very slowly changed to 20 mM $NaPO_4$ (pH 7.8) buffer containing 500 mM NaCl and 1 mM β-ME at a flow-rate of 1 mL/min over 30 min at 4 °C. Proteins then eluted with a slow gradient to 20 mM $NaPO_4$ (pH 7.8), 500 mM NaCl, 50 mM EDTA, and 1 mM β-ME. One milliliter aliquots were collected, and

a chart recorder monitored the protein content based on absorbance of aromatic groups at 280 nm. Fractions that had a sufficient amount of protein were applied to an 8% gel and stained with GelCode blue staining reagent (Pierce, Rockford, IL) and used for further analysis.

Steady-State Fluorescence Measurements. Fluorescence spectra were obtained on a QuantaMaster-4/2003 spectrofluorometer (Photon Technology International, Lawrenceville, NJ) equipped with the QNW-4 rapid temperature control turret. Measurements were performed with a scan speed of 50 nm/min and data intervals of 0.5 nm. Emission was measured in the ratio mode and corrected for the appropriate solvent-blanks, as well as for wavelength-dependent bias of the optics and detection system. Spectra were recorded over the 290−600 nm range in 1 cm quartz cells (NSG Precise Cell Inc., Farmingdale, NY). The fluorescence experiments employed tryptophan and tyrosine residues as intrinsic reporters. Therefore, excitation wavelengths of 280 and 295 nm were used. Each spectrum (averaged over 20 scans) was characterized by the position of the intensity maximum, λ_{max}, and the width of the spectral distribution, $\Delta\lambda_{1/2}$. The position of the emission maximum, $\langle\lambda_{max}\rangle$, was calculated as the intensity-weighted average:

$$\langle\lambda_{max}\rangle = \frac{\sum_i \lambda_i F(\lambda_i)}{\sum_i F(\lambda_i)}$$

where $F(\lambda_i)$ is the fluorescence intensity measured at the emission wavelength λ_i.

Circular Dichroism Measurements. Circular dichroism measurements were acquired on a J-710 spectropolarimeter (JASCO, Japan) equipped with a temperature control system (NESLAB, Newington, NH). The spectropolarimeter was calibrated with (+)-10-camphorsulfonic acid prior to measurements. Far-UV spectra were recorded over 180−260 nm in a 0.05-, 0.1-, and 0.5-cm cells, depending on protein concentrations and solvent composition. Near-UV spectra were obtained over 240−340 nm in a 0.5-cm cell. Measurements were performed with a bandwidth of 1 nm, response time of 0.5 s, and scan speed of 20 nm/min. Each spectrum (the average of 100 scans) was corrected for the appropriate solvent blank and, thereafter, smoothed with J-710 software. Raw data were expressed as molar ellipticity in units of deg·cm^2·dmol^{-1}, which takes into account the peptide concentration, the number of amino acids, and the optical path length (*34*).

DNA Binding Experiments. Oligonucleotides (ODN) used in DNA binding experiments were custom synthesized by Invitrogen Life Technologies (Grand Island, NY). Wild-type double-stranded oligonucleotides (I and II annealed together) with the consensus Ets binding site GGAA were used (WT-ODN). In addition, the experiments were performed with mutated double-stranded oligonucleotides (III and IV annealed together, M-ODN): I, ATGTAGACC**GGAA**GTAACTA; II, TAGTTAC**TTCC**GGTCTACAT; III, ATGTAGACC**GCTA**GTAACTA; IV, TAGTTAC**TAGC**GGTCTACAT.

Oligonucleotides were dissolved in a buffer, containing 10 mM Tris-HCl (pH 8.0), 50 mM NaCl, and 1 mM EDTA. The annealing procedure mixed equal molar mixtures of complementary oligonucleotides, which were incubated at 95, 75, 60, 50, and 40 °C for 5 min at each temperature. Double-stranded oligonucleotides were labeled with γ-^{32}P using T4 kinase (Promega, Madison, WI) according to the manufacturer's protocol.

DNA binding experiments were performed using the gel shift assay (Promega, Madison, WI) with modification of previously published methods (*35*). Recombinant protein and radioactively labeled oligonucleotides were incubated for 20 min at room temperature in the presence of a binding buffer [10 mM Tris-HCl, pH 7.5, 4% glycerol, 1 mM $MgCl_2$, 0.5 mM EDTA, 0.5 mM DTT, 50 mM NaCl, and 0.05 mg/mL poly(dI−dC)·poly(dI−dC)]. The reaction was performed in 10 μL total volume, and the entire mixture was applied to a 6% DNA retardation gel containing 50 mM Tris-HCl (pH 8.3), 45 mM boric acid, and 0.5 mM EDTA (0.5× TBE) for 15 min at 250 V. The gels were dried and autoradiographed.

Solid-phase DNA binding experiments occurred in the plastic ELISA plates coated with 50 ng/well recombinant EWS−FLI1 at room temperature for 1 h. The plate was washed 5 times with PBS. ODN mix in binding buffer (see above) was added to each well (50 μL/well). The plate was incubated for 1 h at room temperature and washed 5 times with PBS. Finally, 100 μL of 1% sodium dodecyl sulfate was added to each well, and the plate was incubated for 10 min at room temperature. Samples were collected, and the radioactivity was counted in a γ counter.

Cell-Free Transcription and Translation. Nuclear lysate from 3×10^9 ESFT cells (TC32 cell line) was prepared and frozen into aliquots at −80 °C. Transcription reactions were performed as reported (*36*) and used nuclear lysate from approximately 3×10^6 cells per reaction. We utilized a reporter construct that expressed luciferase instead of a G-less cassette. Recombinant, refolded EWS−FLI1 was dialyzed at 4 °C into 20 mM Tris-Cl (pH 7.9), 100 mM KCl, 20% glycerol, 0.2 mM EDTA, 0.2 mM PMSF, and 1 mM DTT and added just prior to the nuclear lysate. ODN were dissolved in sterile deionized distilled H_2O (ddH_2O) and added to the transcription mix following the recombinant EWS−FLI1. Transcription occurred at 30 °C for 90 min. The transcription reactions were extracted with 1:1 (v/v) phenol/chloroform and precipitated with 70% 2-propanol. The precipitate was washed with 100% ethanol and dried by evaporation. Precipitates were dissolved in sterile ddH_2O. Translation with rabbit reticulolysate was performed according to the manufacturer's instructions at 30 °C for 90 min (Promega, Inc.). The translation mix was assayed in a luminometer after the addition of luciferase substrate according to the manufacturer's instructions (Promega, Inc.). Statistical analysis was performed with GraphPad InStat software using the Tukey−Kramer multiple comparison test.

RESULTS

Expression and Purification of Recombinant EWS−FLI1. The coding sequence for EWS−FLI1 fusion protein was cloned into a pET28a(+) bacterial expression vector with a carboxy-terminal histidine tag. Recombinant protein was then expressed in *Escherichia coli*. To overcome the codon bias, we chose BL21-CodonPlus(DE3)-RP cells, which contain extra copies of the *argU* and *proL* genes. These genes encode tRNAs that recognize the arginine codons AGA and AGG

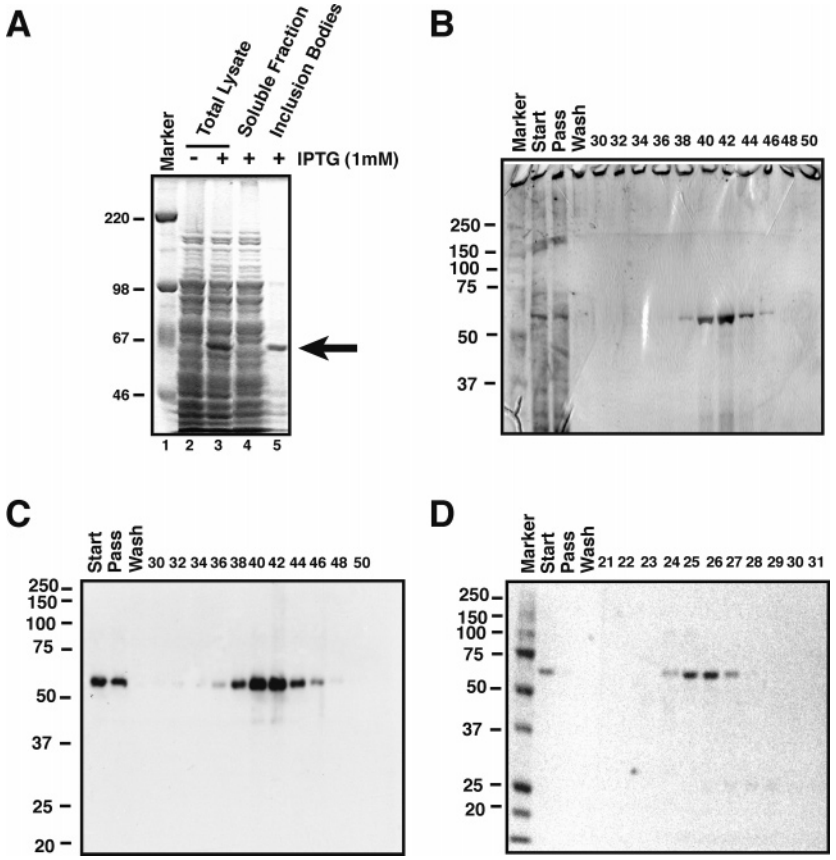

FIGURE 1: Purification and refolding of EWS−FLI1 expressed in BL21-CodonPlus(DE3)-RP bacteria. In panel A, expression from pET28a-(+) vector was induced by 1 mM IPTG. Fractions were resolved on an 8% acrylamide gel and stained with Coomassie blue: total cell lysate (lanes 2, 3), soluble fraction (lane 4), and insoluble fraction containing inclusion bodies (lane 5). The arrow indicates a protein band corresponding to EWS−FLI1. In panel B, the inclusion body fraction was dissolved in 8 M urea and applied to a Ni^+-charged chelating column. Fractions were eluted with a pH gradient, and every other fraction was resolved on an 8% acrylamide gel and silver stained. In panel C, a replica of the gel in panel B was immunoblotted with a FLI1 antibody. In panel D, fractions 38−46 from the initial purification were pooled together and applied to a metal chelating column. Following a refolding protocol, protein fractions were eluted with EDTA, resolved on a 8% acrylamide gel, and stained with GelCode blue.

and the proline codon CCC, respectively. The EWS−FLI1 sequence has six of these rare codons that could limit the expression of full-length molecule in uncompensated *E. coli* strains. Following IPTG induction, a band consistent with EWS−FLI1 (55 kDa) is observed in the total bacterial lysate (Figure 1A, lane 3). When the total bacterial lysate (lane 3) is separated into soluble (Figure 1A, lane 4) and insoluble fractions (Figure 1A, lane 5), the 55 kDa band is found only in the insoluble fraction, corresponding to the inclusion bodies.

Purification of recombinant EWS−FLI1 from inclusion bodies was performed using a conventional chaotropic denaturant as described in Experimental Procedures. First, inclusion bodies were dissolved in 20 mM $NaPO_4$ (pH 7.8), 500 mM NaCl, and 8 M urea and loaded onto a Ni^+-charged chelating affinity column. Following washing to clear nonspecifically bound proteins, samples were eluted with a slow gradient from pH 7.8 to 4.0. This pH-eluted recombinant EWS−FLI1, which is in 8 M urea, will be referred as "purified" throughout the paper. Eluted fractions were resolved on an 8% acrylamide gel, and the proteins were observed by silver staining (Figure 1B). A purification performed with 20 mM $NaPO_4$ (pH 7.8) containing 500 mM NaCl and 6 M GdnHCl also provided similar results (data not shown). This procedure achieved a 60 kDa protein with >95% purity as judged by silver staining. The 60 kDa protein was identified as EWS−FLI1 by immunoblotting with a FLI1 antibody (Figure 1C).

Protein stability under physiological conditions is an important prerequisite of drug development. A number of approaches were utilized to transfer the bacterial-produced EWS−FLI1 into a physiologic buffer, including multiple dialysis strategies (see Experimental Procedures). However, a precipitate was observed with each strategy and very little protein remained in solution (data not shown). Refolding of EWS−FLI1 was achieved following immobilization on a Ni^+-charged chelating chromatography column (see Experimental Procedures). The column solvent was slowly switched from 20 mM $NaPO_4$ (pH 7.8) containing 500 mM NaCl and 8 M urea to 20 mM $NaPO_4$ (pH 7.8) containing 500 mM NaCl and 1 mM β-ME. Following refolding, the recombinant EWS−FLI1 was eluted with 50 mM EDTA in 20 mM $NaPO_4$ (pH 7.8), 500 mM NaCl, and 1 mM β-ME. Fractions were resolved in an 8% acrylamide gel and stained with Coomassie blue (Figure 1D). Eluted fractions 24−27 show a 60 kDa protein, which corresponds to recombinant EWS−FLI1. The EWS−FLI1 obtained following this refolding protocol will be referred to as "refolded" throughout this manuscript. The overall yield of soluble EWS−FLI1 was calculated to be about 0.3−1.2 mg per liter of bacterial culture. Overall, the developed purification and refolding

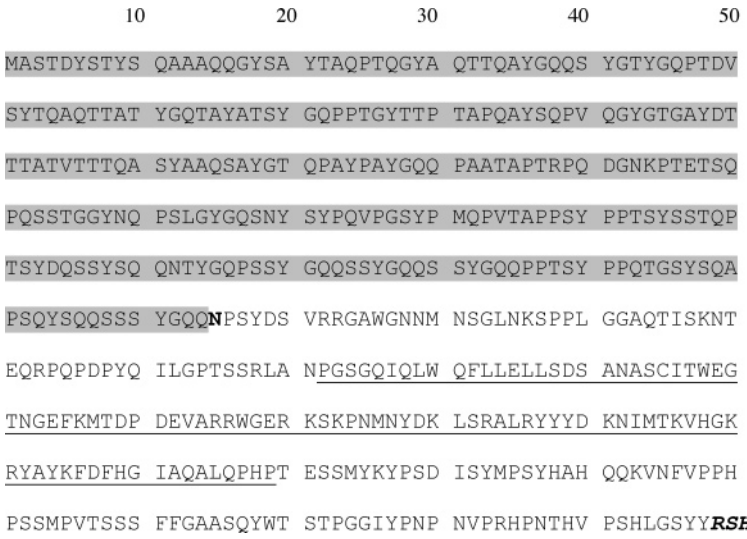

FIGURE 2: Primary sequence of the recombinant EWS−FLI1 expressed in bacteria. Residues 1−264 (gray) are derived from the amino terminus of EWS. N265 (bold) constitutes the connection site. Residues 266−498 are derived from the carboxy terminus of FLI1 protein (residues 220−452). The eight residues on the carboxy terminus of recombinant EWS−FLI1 were added to purify the protein (bold italic). Residues 322−419 (underline) indicate the conserved DNA binding domain in FLI1 protein (*6*).

procedure produces EWS−FLI1 at a concentration of 50−200 μg/mL with 95% purity as estimated by silver staining of acrylamide gels. Furthermore, the recombinant protein under these conditions was stable at 4 °C for 10−15 days as measured by spectroscopic means. Similar results were achieved by eluting recombinant EWS−FLI1 with 1 M imidazole (data not shown).

Structural Assessment of Recombinant EWS−FLI1. The primary sequence of EWS−FLI1 (Figure 2) suggests a protein expected to be largely disordered under native conditions due to the low overall hydrophobicity (*37*). In this regard, we note that globular and disordered proteins occupy nonoverlapping regions in the charge−hydrophobicity plots with natively unfolded proteins being localized within a particular region of charge−hydrophobicity phase space (*38*, *39*). Disordered protein structures can be recognized using the following criterion (*38*, *39*):

$$\langle H \rangle \leq \langle H \rangle_b = \frac{\langle R \rangle + 1.15}{2.79}$$

where $\langle H \rangle$ and $\langle R \rangle$ are the mean hydrophobicity and the mean net charge, respectively, calculated for a given protein and $\langle H \rangle_b$ is the "boundary" mean hydrophobicity, below which a polypeptide chain with a given $\langle R \rangle$ is expected to be disordered. The calculated values for the EWS−FLI1 sequence are $\langle H \rangle = 0.39$, $\langle R \rangle = 0.08$, and $\langle H \rangle_b = 0.42$, indicating that EWS−FLI1 is likely to be largely disordered under relatively native conditions. Furthermore, the amino acid sequence-based calculation of the secondary structure content using the GOR4 method (*40*), HNN predictor algorithm (*41*), or both also indicate that most of the protein chain (∼80%) is expected to approach an unfolded conformation. It appears, therefore, that determination of the 3D structure of EWS−FLI1 at atomic resolution may present a difficult challenge, and other experimental techniques capable of providing the structural information are required.

Secondary Structure by Far-UV CD Spectrum. Refolding of EWS−FLI1 was monitored by circular dichroism (CD). Spectra were recorded for EWS−FLI1 under various thermodynamic conditions, which included protein fractions generated at various stages of purification and refolding. The far-UV CD spectra of the purified and refolded recombinant EWS−FLI1 are shown (Figure 3A, solid and dashed lines, respectively). Purified EWS−FLI1 in 8 M urea (pH 4) exhibits CD spectra that are typical for essentially β-structured polypeptide chains (Figure 3A, solid line). However, the negative minimum at ∼216 nm is rather weak and along with the spectral contributions in the 220−240 nm range might indicate the 229 nm tyrosyl CD band (*42*). EWS−FLI1 contains 52 tyrosine, 5 tryptophan, and 7 phenylalanine residues, and many of these side chains are in close proximity, e.g., YXY repeats (Figure 2). Such aromatic clusters are important since they usually lead to a mixture of optical transitions, thus affecting the CD signal (*43*). Quite similar β-like spectra have been reported on numerous occasions for a number of prion-related peptides (*44*, *45*), proteins in solid state (*46*−*48*), and liquid crystallized polymeric phases (*49*, *50*). In addition, the EWS−FLI1 contains 53 proline residues and therefore might exhibit features of poly(Pro)-type structures (*51*). The far-UV CD band observed for EWS−FLI1 in 8 M urea at pH 4 most likely reflects the apparent β-structures comprising the features of proline-rich macromolecules. However, the stability of this structure under the presence of large amounts of denaturant is unusual and requires further examination.

After refolding, the recombinant EWS−FLI1 protein yields CD spectra (Figure 3A, dashed line) that exhibit hallmarks of an essentially unfolded conformation (*34*). This result agrees well with primary sequence analysis, which indicates only 20% of the residues in α-helical or β-extended configurations. However, more detailed analysis of the far-UV CD spectrum shows that EWS−FLI1, being considerably disordered, still preserves some residual structure. Specifically, the characteristic negative ellipticity at 230 nm points to an apparent mixture of α-helical and β-stranded, random, and poly(Pro)-type forms (*34*, *51*).

Residual Tertiary Structure by Near-UV CD Spectrum. Additional alternations in EWS−FLI1 structure, as caused by the immobilization-assisted refolding, are observed from

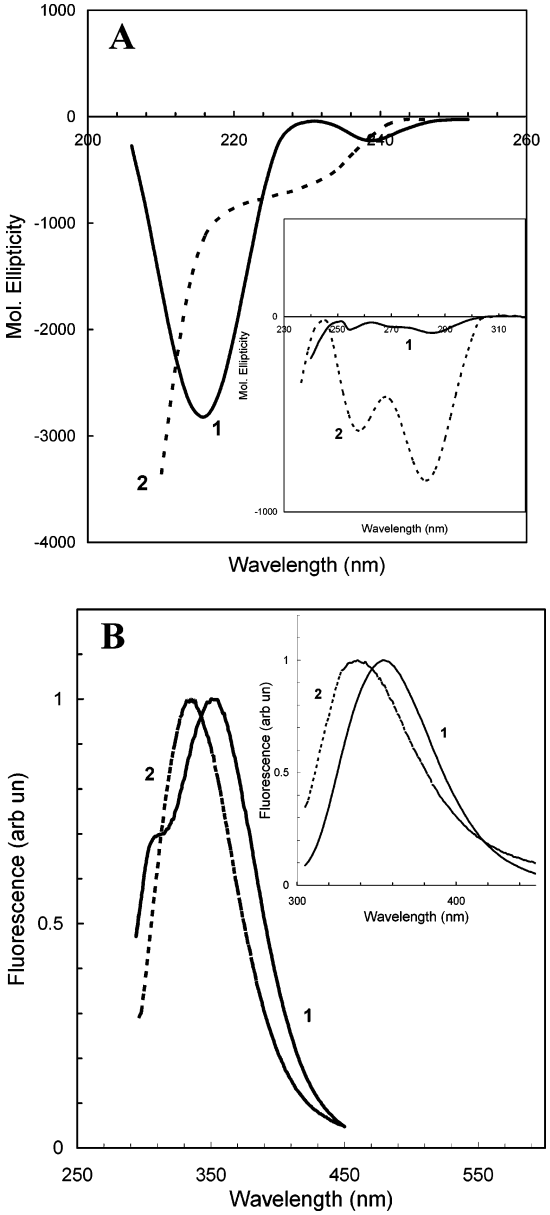

FIGURE 3: Structural properties of recombinant EWS−FLI1. Panel A shows the far-UV circular dichroism spectra of 10 μM purified (1, —) and 3 μM refolded (2, − − −) recombinant EWS−FLI1. Spectra were obtained in a 0.05 cm cell. The inset shows near-UV circular dichroism spectra recorded for the same sample in a 0.5 cm cell. Panel B shows the fluorescence emission spectra of 4 μM purified (1, —) and 1 μM refolded (2, − − −) recombinant EWS−FLI1. Fluorescence was excited at 280 nm, and the spectra were normalized to the intensity at the maximum. The inset shows fluorescence spectra recorded under excitation at 295 nm. Other conditions were as described in Experimental Procedures.

the near-UV CD spectra (Figure 3A, inset). Purified EWS−FLI1 (Figure 3A, inset, solid line) exhibits a lack of ellipticity from 270 to 290 nm. These data indicate that under these conditions the protein aromatic side chains locate in a symmetric environment, that is, are exposed to the solvent (*34*). In contrast, the defined structure based upon the near-UV CD spectra obtained for refolded EWS−FLI1 (Figure 3A, inset, dashed line) indicated that the aromatic side chains exist in an asymmetric environment. This suggests that hydrophobic groups of the refolded protein are buried into the molecular interior.

Residual Structure by Fluorescence. Steady-state fluorescence experiments with varying excitation wavelength provide supplementary evidence for gross conformational rearrangements of EWS−FLI1 following refolding (Figure 3B). Using excitation at 280 nm, we found that the emission spectra of purified EWS−FLI1 (Figure 3B, solid line) center around 350 nm, which is close to that of tryptophan in water (351 nm, ref *52*). Furthermore, the spectra demonstrate a shoulder at 305 nm, which likely corresponds to tyrosine fluorescence. Refolding results in a significant blue shift of the emission spectra (λ_{max} = 335 nm) and is accompanied by quenching of tyrosine fluorescence (Figure 3B, dashed line). Excitation at 295 nm allows for selective measuring of the tryptophan fluorescence (*52*). Since all five tryptophan residues are located in the FLI1 domain, the tryptophan emission spectrum is potentially a probe for FLI1 domain structural rearrangements. These rearrangements are demonstrated vividly since the refolding encourages the collapse of the FLI domain, as indicated by blue shift (∼15 nm) of the tryptophan emission (Figure 3B inset).

Overall, fluorescence and CD experiments demonstrate that recombinant EWS−FLI1 undergoes a major conformational change following refolding. At first, purification of the protein under the denaturing conditions (8 M urea, pH 7.8−4) induces a highly stable intermediate structure that lacks specific tertiary interactions, contains a significant amount of residual secondary structure, and undergoes further refolding under the absence of urea. This captured intermediate comprises the features of β-rich conformations with increased accessibility of nonpolar groups to solvent. Whether this molecular form has relevance to the function of EWS−FLI1 is not clear, but it may play a role in structural integrity. Employing immobilization-assisted refolding allows obtaining the thermodynamically stable molecular form where the protein backbone is essentially unfolded, and aromatic side chains constitute a tight hydrophobic core avoiding their exposure to the polar solvent. Quite similar structural features, that is, lack of the secondary structure under the presence of significant residual tertiary structure, have been reported recently for the carboxy-terminal domain of caldesmon (*53*).

Recombinant EWS−FLI1 Binds to Specific DNA Sequences. EWS−FLI1 retains the DNA binding domain of FLI1 and binds to DNA as shown by previous studies that utilized whole cell extracts or in vitro reticulocyte-translated proteins (*16*, *54*). We wanted to evaluate the DNA binding of both purified and refolded recombinant EWS−FLI1. We performed DNA binding experiments using two different assays. Electromobility shift assays (EMSA) were performed using recombinant EWS−FLI1 and either 20 base-pair wild-type oligodeoxynucleotide (WT-ODN) with a core Ets binding consensus, GGAA, or a mutant oligodeoxynucleotide (M-ODN) with a mutated core to GCTA. Refolded recombinant EWS−FLI1 bound to radioactive labeled WT-ODN is shown by the band shift (Figure 4A, right panel, lane 4). This binding was competed with excess unlabeled WT-ODN (Figure 4A, right panel, lanes 5−9). Binding specificity was confirmed by using radiolabeled M-ODN, which did not bind to EWS−FLI1 (Figure 4A, right panel, lane 2). Unlabeled M-ODN did not compete WT-ODN binding, an expected control observation (Figure 4A, right panel, lanes 10−14).

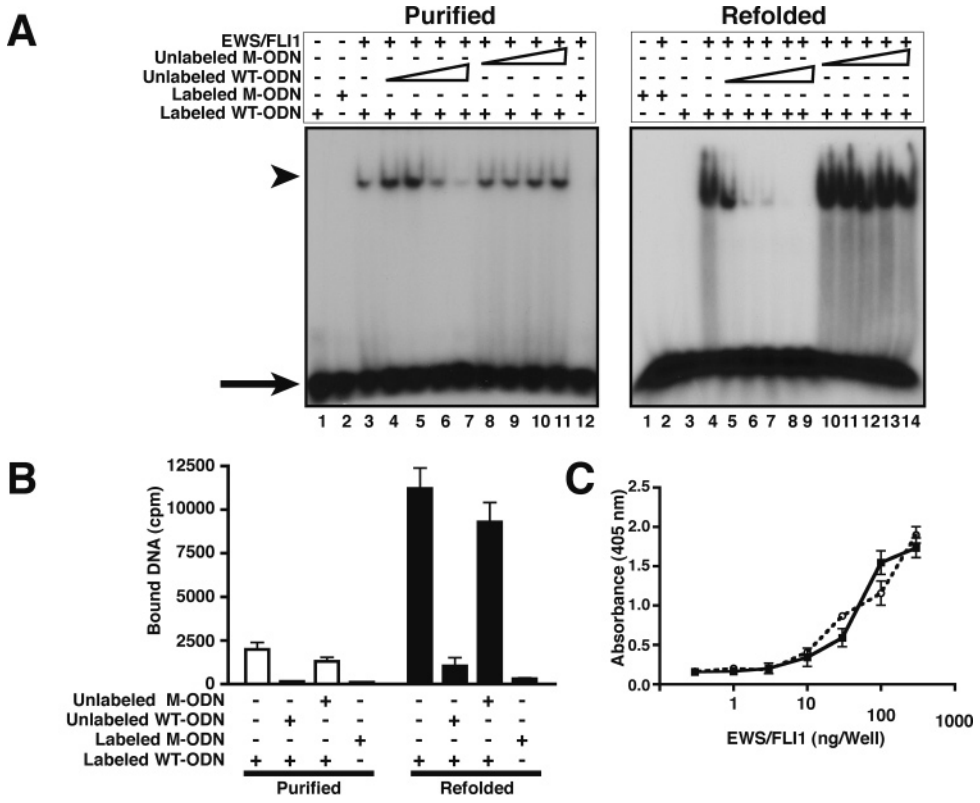

FIGURE 4: Refolded recombinant EWS−FLI1 binds DNA more efficiently than the initial structure protein. In panel A, EWS−FLI1 and ODN complexes were mixed in DNA binding buffer and resolved on 6% DNA retardation gels. Autoradiographs showed free ODNs (arrow) and protein−ODN complexes (arrowhead). The left panel contained 1.5 μM purified EWS−FLI1 mixed with 15 nM ^{32}P-labeled ODN. The right panel contained 40 nM refolded EWS−FLI1 mixed with 15 nM ^{32}P-labeled WT-ODN. Unlabeled ODN competition at increasing concentration is indicated by a triangle. Unlabeled ODN concentrations were 0.15, 0.45, 1.5, and 5 μM for the left panel and 0.15, 0.45, 1.5, 4.5, and 15 μM for right the panel. In panel B, 96-well ELISA plates were coated with 50 ng/well recombinant EWS−FLI1, purified (white bars) and refolded (black bars). The same labeled (8 nM) and unlabeled (6.4 μM) ODN as those used in EMSA were used for protein−DNA binding on the solid surface. After the surface was washed, retained ^{32}P was quantified by a γ counter and plotted on the *Y* axis as counts per minute. In panel C, ELISA plates were coated with indicated amounts of purified EWS−FLI1 (− − −, ○) or refolded EWS−FLI1 (—, ■) and probed with a FLI1 antibody. Each point in the graph represents the mean of triplicate wells. Standard deviation is indicated by error bars.

To address the impact of refolding on the efficiency of DNA binding, we performed similar experiments on the purified EWS−FLI1. To visualize a gel shift, approximately 30-fold more purified protein was required with the WT-ODN than the refolded protein (Figure 4A, left panel compared to right panel). Competition studies of DNA binding showed loss of DNA binding by EWS−FLI1 at the same ratio of EWS−FLI1 to cold WT-ODN (Figure 4A).

DNA binding experiments were also performed on a solid matrix by attaching the recombinant EWS−FLI1 to a plastic surface. ^{32}P-labeled wild-type or mutant ODNs were added to the EWS−FLI1, along with their unlabeled competitions. Refolded EWS−FLI1 bound to radioactive-labeled WT-ODN but not to radioactive-labeled M-ODN (Figure 4B). Similarly, unlabeled WT-ODN competed for binding, while unlabeled M-ODN did not compete (Figure 4B). Purified EWS−FLI1 showed 5-fold less DNA binding than the refolded EWS−FLI1. We considered the possibility that purified EWS−FLI1 may not bind to plastic surface as well as refolded EWS−FLI1 and that this could be the reason for the observed differences in DNA binding. To address this, we quantitatively measured the amount of adherent EWS−FLI1 using ELISA. Our results showed that both recombinant proteins bind to plastic surface with a similar avidity (Figure 4C), suggesting that the difference in DNA binding reflects differences in overall protein structure. All protein−DNA interaction experiments were done at least three times.

Both of these experimental models therefore demonstrated DNA binding by recombinant EWS−FLI1 (Figure 4). DNA binding as measured by EMSA and in solid matrix involves a complex binding solvent (see Experimental Procedures), which might impact protein structure. To address this issue, we recorded the fluorescence spectra of EWS−FLI1 in binding solvent utilizing both the purified and refolded proteins as stock solutions. Using excitation at 280 nm, we found that the emission spectrum of purified protein in binding solvent centers at 331 nm (Figure 5, solid line), whereas that of the refolded protein yields an emission maximum at 326 nm (Figure 5, dashed line). These data indicate that the binding solvent indeed encourages further collapse of the protein chain, avoiding exposure of the aromatic side chains to the solvent. However, the spectroscopic characteristics of tryptophan residues are indistinguishable between both experiments (inset). Since all the tryptophan residues are located in the FLI1 domain, this finding suggests that structural rearrangements of the EWS domain are required to ensure better DNA binding.

Transcriptional Activity of Recombinant EWS−FLI1. A cell-free transcription−translation (CFTT) assay was devel-

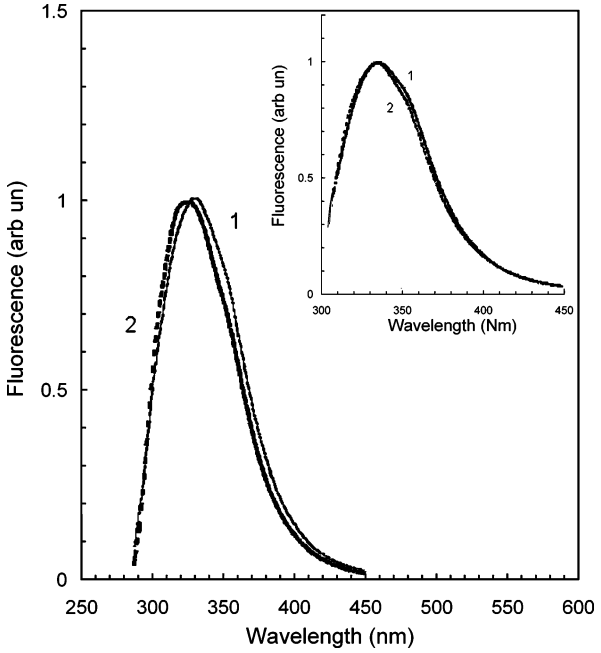

FIGURE 5: Effect of DNA binding buffer upon EWS−FLI1 structure. Fluorescence spectra of purified (1, —) and refolded (2, − − −) recombinant EWS−FLI1 in DNA binding solvent. Fluorescence was excited at 280 nm, and the spectra were normalized to the intensity at the maximum. The inset shows the spectra recorded under excitation at 295 nm of purified (1, —) and refolded (2, − − −). Other conditions were as described in Experimental Procedures.

oped to test the functional activity of recombinant EWS−FLI1. An established EWS−FLI1 responsive promoter, the Id2 luciferase reporter, allowed for EWS−FLI1-initiated transcription. The luciferase mRNA was translated into luciferase protein for quantitative analysis of message (*8*, *9*). The transcription assay was linear based on increasing amounts of CMV−luciferase plasmid DNA from 5 to 100 ng of plasmid (data not shown). The translation assay was linear from 1 to 20000 pg of luciferase mRNA (data not shown). Since the transcription assay was exquisitely sensitive to changes in reaction buffer conditions, refolded, recombinant EWS−FLI1 was first dialyzed into the transcription reaction buffer. Since purified EWS−FLI1 precipitated during dialysis, it could not be used in this assay.

Refolded EWS−FLI1 increased the Id2 promoter activity by 3.5-fold compared to background activity of nuclear lysate alone (Figure 6, column 1 vs 2, $p < 0.01$). To ensure that promoter activation was due to recombinant EWS−FLI1, EWS−FLI1 activity was competed with WT-ODN in the transcription reaction. WT-ODN reduced the transcriptional activity to 20% of control (Figure 6, lane 3 vs 2, $p = < 0.001$), while M-ODN did not significantly affect transcriptional activity (Figure 6, lane 4 vs 2). A CMV promoter, which is not activated by EWS−FLI1, upstream of a luciferase gene assessed the specificity of transcript initiation (data not shown). The CMV promoter was not activated by recombinant EWS−FLI1 (Figure 6, column 5 vs 6). These results suggest that in addition to DNA binding, refolded recombinant EWS−FLI1 also activates transcription in a sequence-specific fashion.

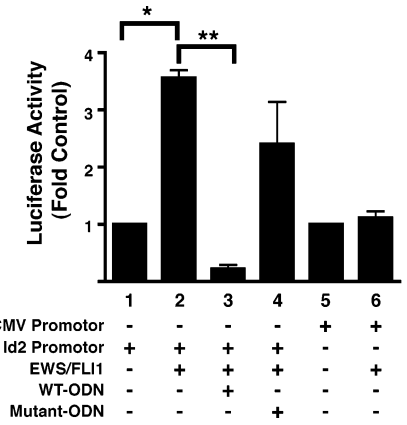

FIGURE 6: Recombinant EWS−FLI1 activates Id2 promoter. Recombinant refolded EWS−FLI1 was evaluated in a cell-free transcription−translation assay (Experimental Procedures) by adding recombinant protein into a reaction mixture of nuclear lysate and reporter plasmid: background Id2 promoter activation (lane 1), Id2 plus EWS−FLI1 (lane 2), Id2 plus EWS−FLI1 and WT-ODN (lane 3), Id2 plus EWS−FLI1 and M-ODN (lane 4), background CMV promoter (lane 5), and CMV plus EWS−FLI1 (lane 6). Significant differences between groups were determined by Tukey−Kramer multiple comparison test (∗, $p < 0.01$; ∗∗, $p < 0.001$). Experiments were performed twice in duplicates, and a representative one is presented.

DISCUSSION

EWS−FLI1 is an important target for developing novel therapeutics for ESFT due to its selective expression and critical function in tumor cells. Antitumor agents that specifically inactivate EWS−FLI1 will likely improve the therapy for patients suffering from ESFT. Expression and purification of EWS−FLI1 provided many technical challenges due to the solubility and stability of the protein. Initial attempts to produce EWS−FLI1 demonstrated that the protein was insoluble and located in the bacterial inclusion bodies. In SF9 insect cells, recombinant EWS−FLI1 also accumulated as insoluble aggregates. Expression of EWS−FLI1 in mammalian cells with a signal peptide for secretion into the conditioned media was also unsuccessful. Even though mammalian cells expressed some EWS−FLI1, there was no detectable EWS−FLI1 in the conditioned media. A similar approach directing export of EWS−FLI1 to the periplasmic space of bacteria was unsuccessful. Eventually recombinant EWS−FLI1 protein was produced with appropriate biological activity that can be purified from the inclusion bodies of *E. coli* bacteria in two steps, purification in the presence of 8 M urea followed by immobilization-assisted refolding into physiological buffer. Since EWS−FLI1 is not glycosylated (*55*) and there have been no reports of EWS−FLI1 type 1 being phosphorylated, we expressed this human protein in bacteria.

EWS−FLI1 provides investigators an opportunity to exploit a unique molecular target to improve cancer therapy. Current strategies identify small molecule lead compounds that bind to protein targets by screening arrays of various sorts (*56*). Lead compounds are also identified upon the basis of predicted 3-D structures (*57*, *58*). Once the 3-D structure is determined, custom design of small molecules against selected domains can proceed. Structural assessment revealed that after being refolded in vitro, EWS−FLI1 has nearly normal structural and binding properties as shown by CD

and fluorescence spectroscopy together with the biologic assays. Interestingly, despite the low content of ordered secondary structure (far-UV CD), the residual structure of recombinant protein is relatively well organized (near-UV CD, fluorescence). Since the structure of EWS−FLI1 is currently unresolved, molecular assays were used to determine whether the EWS−FLI1 that we produced has functional properties.

To explore the molecular activity of the chimeric oncoprotein, we developed several functional assays including a novel CFTT method that allows probing the transcriptional activity of recombinant EWS−FLI1. In this regard, both CFTT and DNA binding experiments strongly supported the conclusion that recombinant EWS−FLI1 expressed in bacteria is a functional protein. DNA binding of purified recombinant EWS−FLI1 was unexpected, although it was significantly less than refolded EWS−FLI1. It is possible that a small fraction of purified EWS−FLI1 may be refolding in the DNA binding buffer. Furthermore, when DNA binding abilities of purified vs refolded proteins are compared, the difference was 30-fold in EMSA but 5-fold in solid-phase assays. Immobilization of purified protein to a chelating column enabled the maximum refolding in our methodology. Similarly, binding the purified protein to a plastic surface followed by buffer switch to DNA binding buffer may result in a larger fraction of purified EWS−FLI1 being refolded. Alternatively, the formation of a tight protein−DNA complex may lead to minimal folding of the disordered protein. In this situation, the binding of EWS−FLI1 to DNA would be a local binding, encompassing a rather limited sequence of protein (e.g., FLI domain) rather than overall binding. On the other hand, recombinant EWS−FLI1 may be an example of the induced-fit model for DNA site-recognition in which unordered or poorly ordered regions of the protein become ordered upon binding to DNA. More extensive studies on the EWS−FLI1−DNA and EWS−FLI1−protein interactions will be a logical extension of this work. A method of testing these molecular activities of EWS−FLI1 was necessary to test a function of the recombinant protein.

Cell-free models of transcription have been extremely informative of the transcriptome molecular biology (*59*). These models have relied on either fully recombinant or extracted nuclear proteins for transcriptional reconstitution. Assay of these systems utilized a "G-less" cassette to measure the rate and quantity of RNA produced as the output of transcriptional activity (*36*). The CFTT assay developed in this study utilizes nuclear extract from ESFT cells to ensure the presence of cotranscriptional activators for EWS−FLI1 (*60*, *61*). Since experiments compared baseline transcription with added recombinant EWS−FLI1, differences due to the recombinant protein were measured. Careful attention was paid to ensure the linearity of the system over the ranges studied. The use of luciferase rather than the G-less cassette allowed for a sensitive and nonradioactive quantitative readout. The CFTT could be applicable to many transcription factors and allow for the development of assays to evaluate compounds that modulate EWS−FLI1 activity. Unfortunately, there are likely EWS−FLI1 functions such as splicing that our assay could not assess (*20*, *21*). Likewise, the oncogenic function of EWS−FLI1 can be independent of DNA binding (*62*).

In summary, recombinant EWS−FLI1 can be purified from bacteria in two steps: first, purification in urea and, second, refolding with the recombinant protein immobilized on an affinity column. The structure of recombinant EWS−FLI1 in solution under various thermodynamic conditions was evaluated and revealed gross conformational changes within EWS−FLI1 protein as a result of the refolding process. Recombinant EWS−FLI1 bound to DNA with the predicted sequence specificity. Finally, a novel CFTT assay demonstrated functional activity of recombinant EWS−FLI1. These studies will lead to a better understanding of the oncogenic function of fusion transcription factors and may lead to the development of novel therapeutic agents for patients with ESFT.

ACKNOWLEDGMENT

We would like to thank Drs. Angela M. Gronenborn, Jim Carney, and Joe Fondell for helpful discussions, reagents, and equipment. The Id2 promoter was kindly provided by Dr. Takashi Tokino. Amy Skversky, Naamah Zitomersky, and Sarah Zaidi provided excellent technical support.

REFERENCES

1. Grier, H. E., Krailo, M. D., Tarbell, N. J., Link, M. P., Fryer, C. J., Pritchard, D. J., Gebhardt, M. C., Dickman, P. S., Perlman, E. J., Meyers, P. A., Donaldson, S. S., Moore, S., Rausen, A. R., Vietti, T. J., and Miser, J. S. (2003) Addition of ifosfamide and etoposide to standard chemotherapy for Ewing's sarcoma and primitive neuroectodermal tumor of bone, *N. Engl. J. Med. 348*, 694−701.
2. Meyers, P. A., Krailo, M. D., Ladanyi, M., Chan, K. W., Sailer, S. L., Dickman, P. S., Baker, D. L., Davis, J. H., Gerbing, R. B., Grovas, A., Herzog, C. E., Lindsley, K. L., Liu-Mares, W., Nachman, J. B., Sieger, L., Wadman, J., and Gorlick, R. G. (2001) High-dose melphalan, etoposide, total-body irradiation, and autologous stem-cell reconstitution as consolidation therapy for high-risk Ewing's sarcoma does not improve prognosis, *J. Clin. Oncol. 19*, 2812−2820.
3. Delattre, O., Zucman, J., Plougastel, B., Desmaze, C., Melot, T., Peter, M., Kovar, H., Joubert, I., de Jong, P., Rouleau, G., Aurias, A., and Thomas, G. (1992) Gene fusion with an ETS DNA-binding domain caused by chromosome translocation in human tumours, *Nature 359*, 162−165.
4. May, W. A., and Denny, C. T. (1997) Biology of EWS/FLI and related fusion genes in Ewing's sarcoma and primitive neuroectodermal tumor, *Curr. Top. Microbiol. Immunol. 220*, 143−150.
5. de Alava, E., and Gerald, W. L. (2000) Molecular biology of the Ewing's sarcoma/primitive neuroectodermal tumor family, *J. Clin. Oncol. 18*, 204−213.
6. Karim, F. D., Urness, L. D., Thummel, C. S., Klemsz, M. J., McKercher, S. R., Celada, A., Van Beveren, C., Maki, R. A., Gunther, C. V., Nye, J. A., and Graves, B. J. (1990) The ETS-domain: a new DNA-binding motif that recognizes a purine-rich core DNA sequence, *Genes Dev. 4*, 1451−1453.
7. Hahm, K. B., Cho, K., Lee, C., Im, Y. H., Chang, J., Choi, S. G., Sorensen, P. H., Thiele, C. J., and Kim, S. J. (1999) Repression of the gene encoding the TGF-beta type II receptor is a major target of the EWS−FLI1 oncoprotein, *Nat. Genet. 23*, 222−227.
8. Fukuma, M., Okita, H., Hata, J., and Umezawa, A. (2003) Upregulation of Id2, an oncogenic helix-loop-helix protein, is mediated by the chimeric EWS/ets protein in Ewing sarcoma, *Oncogene 22*, 1−9.
9. Nishimori, H., Sasaki, Y., Yoshida, K., Irifune, H., Zembutsu, H., Tanaka, T., Aoyama, T., Hosaka, T., Kawaguchi, S., Wada, T., Hata, J., Toguchida, J., Nakamura, Y., and Tokino, T. (2002) The Id2 gene is a novel target of transcriptional activation by EWS-ETS fusion proteins in Ewing family tumors, *Oncogene 21*, 8302−8309.
10. Nakatani, F., Tanaka, K., Sakimura, R., Matsumoto, Y., Matsunobu, T., Li, X., Hanada, M., Okada, T., and Iwamoto, Y. (2003)

Identification of p21WAF1/CIP1 as a direct target of EWS−Fli1 oncogenic fusion protein, *J. Biol. Chem. 278*, 15105−15115.
11. Abaan, O. D., Levenson, A., Uren, A., and Toretsky, J. A. The protein tyrosine phosphatase PTPL1 modulates Ewing's sarcoma tumorigenesis, *Oncogene*, in press.
12. Watanabe, G., Nishimori, H., Irifune, H., Sasaki, Y., Ishida, S., Zembutsu, H., Tanaka, T., Kawaguchi, S., Wada, T., Hata, J., Kusakabe, M., Yoshida, K., Nakamura, Y., and Tokino, T. (2003) Induction of tenascin-C by tumor-specific EWS-ETS fusion genes, *Genes, Chromosomes Cancer 36*, 224−232.
13. Thompson, A. D., Braun, B. S., Arvand, A., Stewart, S. D., May, W. A., Chen, E., Korenberg, J., and Denny, C. (1996) EAT-2 is a novel SH2 domain containing protein that is up regulated by Ewing's sarcoma EWS/FLI1 fusion gene, *Oncogene 13*, 2649−2658.
14. Arvand, A., Bastians, H., Welford, S. M., Thompson, A. D., Ruderman, J. V., and Denny, C. T. (1998) EWS/FLI1 up regulates mE2-C, a cyclin-selective ubiquitin conjugating enzyme involved in cyclin B destruction, *Oncogene 17*, 2039−2045.
15. May, W. A., Arvand, A., Thompson, A. D., Braun, B. S., Wright, M., and Denny, C. T. (1997) EWS/FLI1-induced manic fringe renders NIH 3T3 cells tumorigenic, *Nat. Genet. 17*, 495−497.
16. Bailly, R. A., Bosselut, R., Zucman, J., Cormier, F., Delattre, O., Roussel, M., Thomas, G., and Ghysdael, J. (1994) DNA-binding and transcriptional activation properties of the EWS−FLI-1 fusion protein resulting from the t(11;22) translocation in Ewing sarcoma, *Mol. Cell. Biol. 14*, 3230−3241.
17. Zwerner, J. P., and May, W. A. (2001) PDGF-C is an EWS/FLI induced transforming growth factor in Ewing family tumors, *Oncogene 20*, 626−633.
18. Dauphinot, L., De Oliveira, C., Melot, T., Sevenet, N., Thomas, V., Weissman, B. E., and Delattre, O. (2001) Analysis of the expression of cell cycle regulators in Ewing cell lines: EWS−FLI-1 modulates p57KIP2 and c-Myc expression, *Oncogene 20*, 3258−3265.
19. Deneen, B., Welford, S. M., Ho, T., Hernandez, F., Kurland, I., and Denny, C. T. (2003) PIM3 proto-oncogene kinase is a common transcriptional target of divergent EWS/ETS oncoproteins, *Mol. Cell. Biol. 23*, 3897−3908.
20. Knoop, L. L., and Baker, S. J. (2000) The splicing factor U1C represses EWS/FLI-mediated transactivation, *J. Biol. Chem. 275*, 24865−24871.
21. Knoop, L. L., and Baker, S. J. (2001) EWS/FLI alters 5′-splice site selection, *J. Biol. Chem. 276*, 22317−22322.
22. May, W. A., Gishizky, M. L., Lessnick, S. L., Lunsford, L. B., Lewis, B. C., Delattre, O., Zucman, J., Thomas, G., and Denny, C. T. (1993) Ewing sarcoma 11;22 translocation produces a chimeric transcription factor that requires the DNA-binding domain encoded by FLI1 for transformation, *Proc. Natl. Acad. Sci. U.S.A. 90*, 5752−5756.
23. Dohjima, T., Lee, N. S., Li, H., Ohno, T., and Rossi, J. J. (2003) Small interfering RNAs expressed from a Pol III promoter suppress the EWS/Fli-1 transcript in an Ewing sarcoma cell line, *Mol. Ther. 7*, 811−816.
24. Tanaka, K., Iwakuma, T., Harimaya, K., Sato, H., and Iwamoto, Y. (1997) EWS−Fli1 antisense oligodeoxynucleotide inhibits proliferation of human Ewing's sarcoma and primitive neuroectodermal tumor cells, *J. Clin. Invest. 99*, 239−247.
25. Toretsky, J. A., Connell, Y., Neckers, L., and Bhat, N. K. (1997) Inhibition of EWS−FLI-1 fusion protein with antisense oligodeoxynucleotides, *J. Neurooncol. 31*, 9−16.
26. Edelhoch, H. (1967) Spectroscopic determination of tryptophan and tyrosine in proteins, *Biochemistry 6*, 1948−1954.
27. Gill, S. C., and von Hippel, P. H. (1989) Calculation of protein extinction coefficients from amino acid sequence data, *Anal. Biochem. 182*, 319−326.
28. Mateo-Lozano, S., Tirado, O. M., and Notario, V. (2003) Rapamycin induces the fusion-type independent downregulation of the EWS/FLI-1 proteins and inhibits Ewing's sarcoma cell proliferation, *Oncogene 22*, 9282−9287.
29. Mukhopadhyay, A. (1997) Inclusion bodies and purification of proteins in biologically active forms, *Adv. Biochem. Eng. Biotechnol. 56*, 61−109.
30. (1993) Metal-Chelating Affinity Chromatography. *Current Protocols in Molecular Biology*; (Ausubel, F. M., Brent, R., Kingston, R. E., Moore, D. D., Seidman, J. G., Smith, J. A., and Struhl, K., Eds.) Vol. 2, p 10.11.18, John Wiley & Sons Inc., New York.
31. Cohen, D. R. (2000) Expression and purification of histidine-tagged transcription factors, *Methods Mol. Biol. 130*, 203−225.
32. Uren, A., Reichsman, F., Anest, V., Taylor, W. G., Muraiso, K., Bottaro, D. P., Cumberledge, S., and Rubin, J. S. (2000) Secreted frizzled-related protein-1 binds directly to Wingless and is a biphasic modulator of Wnt signaling, *J. Biol. Chem. 275*, 4374−4382.
33. Chaudhuri, J. B. (1994) Refolding recombinant proteins: process strategies and novel approaches, *Ann. N.Y. Acad. Sci. 721*, 374−385.
34. Woody, R. W. (1996) *Circular Dichorism and the Conformational Analysis of Biomolecules*, Plenum Press, New York.
35. Molloy, P. L. (2000) Electrophoretic mobility shift assays, *Methods Mol. Biol. 130*, 235−246.
36. Fondell, J. D. (2002) Gene activation by thyroid hormone receptor in vitro and purification of the TRAP coactivator complex, *Methods Mol. Biol. 202*, 195−214.
37. Miyazawa, S., and Jernigan, R. L. (1985) Estimation of Effective Interresidue Contact Energies from Protein Crystal Structures: Quasi-Chemical Approximation, *Macromolecules 18*, 534−552.
38. Uversky, V. N. (2002) What does it mean to be natively unfolded? *Eur. J. Biochem. 269*, 2−12.
39. Uversky, V. N., Gillespie, J. R., and Fink, A. L. (2000) Why are "natively unfolded" proteins unstructured under physiologic conditions? *Proteins 41*, 415−427.
40. Garnier, J., Gibrat, J. F., and Robson, B. (1996) *Methods in Enzymology*, Vol. 266, p 540−553, Academic Press, San Diego, CA.
41. Guermeur, Y. (1997) Combinaison de classifieurs statistiques, Application a la prediction de structure secondaire des proteins. Ph.D. Thesis, University of Pierre and Marie Curie, Paris, France.
42. Thompson, T. M., Mark, B. L., Gray, C. W., Terwilliger, T. C., Sreerama, N., Woody, R. W., and Gray, D. M. (1998) Circular dichroism and electron microscopy of a core Y61F mutant of the F1 gene 5 single-stranded DNA-binding protein and theoretical analysis of CD spectra of four Tyr → Phe substitutions, *Biochemistry 37*, 7463−7477.
43. Sreerama, N., Manning, M. C., Powers, M. E., Zhang, J. X., Goldenberg, D. P., and Woody, R. W. (1999) Tyrosine, phenylalanine, and disulfide contributions to the circular dichroism of proteins: circular dichroism spectra of wild-type and mutant bovine pancreatic trypsin inhibitor, *Biochemistry 38*, 10814−10822.
44. Ragg, E., Tagliavini, F., Malesani, P., Monticelli, L., Bugiani, O., Forloni, G., and Salmona, M. (1999) Determination of solution conformations of PrP106−126, a neurotoxic fragment of prion protein, by 1H NMR and restrained molecular dynamics, *Eur. J. Biochem. 266*, 1192−1201.
45. Tcherkasskaya, O., Sanders, W., Chynwat, V., Davidson, E. A., and Orser, C. S. (2003) The role of hydrophobic interactions in amyloidogenesis: example of prion-related polypeptides, *J. Biomol. Struct. Dyn. 21*, 353−365.
46. Padrick, S. B., and Miranker, A. D. (2002) Islet amyloid: phase partitioning and secondary nucleation are central to the mechanism of fibrillogenesis, *Biochemistry 41*, 4694−4703.
47. Jourdan, M., Griffiths-Jones, S. R., and Searle, M. S. (2000) Folding of a beta-hairpin peptide derived from the N-terminus of ubiquitin. Conformational preferences of beta-turn residues dictate non-native beta-strand interactions, *Eur. J. Biochem. 267*, 3539−3548.
48. Hu, H. Y., Li, Q., Cheng, H. C., and Du, H. N. (2001) Beta-sheet structure formation of proteins in solid state as revealed by circular dichroism spectroscopy, *Biopolymers 62*, 15−21.
49. Goodman, M., Bhumralkar, Jefferson, E. A., Kwak, J., and Locardi, E. (1998) Collagen mimetics, *Biopolymers 47*, 127−142.
50. Kuball, H. G., and Hofer, T. (2000) Chirality and circular dichroism of oriented molecules and anisotropic phases, *Chirality 12*, 278−286.
51. Sreerama, N., and Woody, R. W. (2003) Structural composition of betaI- and betaII-proteins, *Protein Sci. 12*, 384−388.
52. Konev, S. V. (1967) *Fluorescence and Phosphorescence of Proteins and Nucleic Acids*, Plenum Press, New York.
53. Permyakov, S. E., Millett, I. S., Doniach, S., Permyakov, E. A., and Uversky, V. N. (2003) Natively unfolded C-terminal domain of caldesmon remains substantially unstructured after the effective binding to calmodulin, *Proteins 53*, 855−862.
54. Mao, X., Miesfeldt, S., Yang, H., Leiden, J. M., and Thompson, C. B. (1994) The FLI-1 and chimeric EWS−FLI-1 oncoproteins display similar DNA binding specificities, *J. Biol. Chem. 269*, 18216−18222.

55. Wang, M., Xie, Y., Girnita, L., Nilsson, G., Dricu, A., Wejde, J., and Larsson, O. (1999) Regulatory role of mevalonate and N-linked glycosylation in proliferation and expression of the EWS/FLI-1 fusion protein in Ewing's sarcoma cells, *Exp. Cell Res. 246*, 38−46.
56. Sawyer, T. K. (2004) Cancer metastasis therapeutic targets and drug discovery: emerging small-molecule protein kinase inhibitors, *Expert Opin. Invest. Drugs 13*, 1−19.
57. Gussio, R., Pattabiraman, N., Zaharevitz, D. W., Kellogg, G. E., Topol, I. A., Rice, W. G., Schaeffer, C. A., Erickson, J. W., and Burt, S. K. (1996) All-atom models for the nonnucleoside binding site of HIV-1 reverse transcriptase complexed with inhibitors: a 3D QSAR approach, *J. Med. Chem. 39*, 1645−1650.
58. Chen, H. F., Dong, X. C., Zen, B. S., Gao, K., Yuan, S. G., Panaye, A., Doucet, J. P., and Fan, B. T. (2003) Virtual screening and rational drug design method using structure generation system based on 3D-QSAR and docking, *SAR QSAR Environ. Res. 14*, 251−264.
59. Zhang, H., Iler, N., and Abate-Shen, C. (1996) Rigorous and quantitative assay of transcription in vitro, *Methods Enzymol 273*, 86−99.
60. Watson, D. K., Robinson, L., Hodge, D. R., Kola, I., Papas, T. S., and Seth, A. (1997) FLI1 and EWS−FLI1 function as ternary complex factors and ELK1 and SAP1a function as ternary and quaternary complex factors on the Egr1 promoter serum response elements, *Oncogene 14*, 213−221.
61. Fuchs, B., Inwards, C. Y., and Janknecht, R. (2003) Upregulation of the matrix metalloproteinase-1 gene by the Ewing's sarcoma associated EWS-ER81 and EWS−Fli-1 oncoproteins, c-Jun and p300, *FEBS Lett. 553*, 104−108.
62. Jaishankar, S., Zhang, J., Roussel, M. F., and Baker, S. J. (1999) Transforming activity of EWS/FLI is not strictly dependent upon DNA-binding activity, *Oncogene 18*, 5592−5597.

BI048776Q